

ACCOUNTS OF CHEMICAL RESEARCH

VOLUME 4 NUMBER 11 NOVEMBER, 1971

Interference Effects in Molecular Fluorescence

RICHARD N. ZARE

Department of Chemistry, Columbia University, New York, New York 10027

Received January 27, 1971

Fluorescence studies of molecules have long been a useful and practical tool in elucidating molecular structure and the nature of radiative processes. Ever since the pioneering work of Wood,¹ particular attention has been given to the so-called *resonance fluorescence* of molecular vapors. If a molecular gas at low pressure is irradiated with light that overlaps an absorption line, the molecule makes a transition to a particular quantum level of the excited state. In the absence of collisions, the molecule emits a strikingly simple spectrum consisting of a series of lines, as the molecule falls down to the different quantum levels of the ground state allowed by the electric dipole selection rules. Perhaps the most widely known example of this phenomenon is the excitation of I₂ by the 5461-Å Hg green line, which causes the molecule to emit a progression of closely spaced rotational doublets extending from the visible into the infrared. Thus, molecular resonance fluorescence has a great appeal to chemists for it acts as a "Maxwell's demon," isolating one excited-state level for study.

The calculation of the fluorescent intensity of an ensemble of molecules is based on the concept of stationary states. If the distribution of molecules over the stationary states is known, the intensity of each spectral line is usually given by the product of the population of the stationary state and the transition probability between the upper and lower states under consideration. However, I wish to describe a class of experiments for which knowledge of the stationary-state populations is insufficient to determine the fluorescent line intensities. Instead, it is necessary to know the correlation between the populations of the different excited states in addition to the molecular distribution over the stationary states. These correlations are caused by the particular mode of formation which "locks in" phase relations among the excited-state levels. The presence of these phase relations causes the spatial distribution of the fluorescence to be anisotropic. By applying some external field, *e.g.*, electric, magnetic, rf, it is then possible with the appropriate geometry to alter or destroy these phase relations. The consequent change of the fluorescent intensity of the radiation pattern permits the determination of excited-state parameters, such as the radiative lifetime, the electric dipole moment, the magnetic moment,

and various and sundry fine and hyperfine structure splittings, which are notoriously difficult to measure by other means for such short-lived species.

In atomic spectroscopy, interference effects in atomic fluorescence have been exploited for many years to measure radiative lifetimes and atomic excited-state coupling constants,² but the possibilities are only beginning to be realized in molecular spectroscopy. A partial list of molecules that have already been studied by these interference methods includes H₂,³ OH and OD,⁴ CO,⁵ NO,⁶ CS,⁷ Na₂,⁸ CS₂,⁹ and SO₂.¹⁰ Rather than dwell upon the particulars of each experiment (see Table I), I wish to emphasize here the underlying theoretical foundation that is common to all these studies in hopes that you can then assess the potential and merits of these interference techniques.

The Hanle Effect

One of the first observations of interference effects in fluorescence and how these effects are altered by the application of external fields was made by Hanle almost half a century ago.¹¹ He studied the magnetic depolarization of the atomic fluorescence of mercury vapor excited by 2537-Å resonance radiation. This experiment serves as a prototype in explaining all fluorescence interference effects. A typical Hanle-effect setup is shown in Figure 1. A beam of resonance radiation is linearly polarized at right angles to the direction of a variable magnetic field *H*. The fluo-

(2) For a review, consult B. Budick, *Advan. At. Mol. Phys.*, **3**, 73 (1967).

(3) F. W. Dalby and J. van der Linde, *Colloque Ampère XV*, North-Holland Publishing Co., Amsterdam, 1969; J. van der Linde, Ph.D. Thesis, University of British Columbia, Vancouver, Canada, 1970 (unpublished).

(4) A. Marshall, R. L. deZafra, and H. Metcalf, *Phys. Rev. Lett.*, **22**, 445 (1969); R. L. deZafra and H. Metcalf, *Bull. Amer. Phys. Soc.*, **15**, 83, 563 (1970); R. L. deZafra, A. Marshall, and H. Metcalf, *Phys. Rev. A*, **3**, 1557 (1971); K. R. German and R. N. Zare, *ibid.*, **186**, 9 (1969); *Phys. Rev. Lett.*, **23**, 1207 (1969); *Bull. Amer. Phys. Soc.*, **15**, 82 (1970); K. R. German, T. H. Bergeman, and R. N. Zare, *Phys. Rev.*, submitted for publication.

(5) R. Isler and W. Wells, *Bull. Amer. Phys. Soc.*, **14**, 622 (1969).

(6) G. Gouedard and J.-C. Lehmann, *C. R. Acad. Sci., Ser. B*, **270**, 1664 (1970); K. R. German, R. N. Zare, and D. R. Crosley, *J. Chem. Phys.*, **54**, 4039 (1971).

(7) S. J. Silvers, T. H. Bergeman, and W. Klemperer, *ibid.*, **52**, 4385 (1970); R. W. Field and T. H. Bergeman, *ibid.*, **54**, 2936 (1971).

(8) M. McClintock, W. Demtröder, and R. N. Zare, *ibid.*, **51**, 5509 (1969).

(9) J. W. Mills and R. N. Zare, *Chem. Phys. Lett.*, **5**, 37 (1970).

(10) H. M. Poland and R. N. Zare, *Bull. Amer. Phys. Soc.*, **15**, 347 (1970).

(11) W. Hanle, *Z. Phys.*, **30**, 93 (1924).

(1) See R. W. Wood, "Physical Optics," 3rd ed, Macmillan, New York, N. Y., 1934.

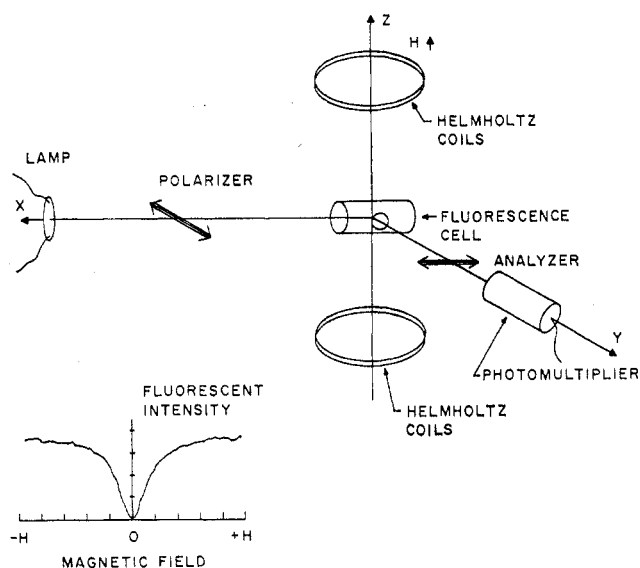


Figure 1. Typical geometrical arrangement of apparatus used in a Hanle-effect experiment. Both polarizer and analyzer are oriented to transmit the electric vector of the light at right angles to the magnetic field. The fluorescent light intensity is recorded as a function of magnetic field strength. A resonance curve as shown in the inset is obtained.

Table I

Molecular Level Crossing and Optical Radiofrequency Double-Resonance Experiments to Date⁸⁻¹⁰

| Molecule | Electronic state | Excitation source | Directly measured quantity |
|-----------------|-----------------------------------|--|--|
| H ₂ | 3d ¹ Σ | Radiofrequency-driven electric discharge | (gτ) _{vJ} |
| OH, OD | A ² Σ ⁺ | Atomic line coincidence | (gτ) _{vJ} |
| | | Molecular resonance lamp | g _F hfs splitting |
| CO | A ¹ Π | Molecular resonance lamp | (gτ) _{av} |
| NO | A ² Σ ⁺ | Atomic line coincidence | (gτ) _{vJ} |
| CS | A ¹ Π | Atomic line coincidence | (gτ) _{vJ} |
| Na ₂ | B ³ Π _u | Laser line coincidence | $\frac{\mu_J}{\Lambda}$ -type doubling (gτ) _{vJ} |
| CS ₂ | V system | White light | (gτ) _{av} |
| SO ₂ | A (¹ B ₁) | White light | (gτ) _{av} |

rescent light is detected in a direction parallel to the electric vector \mathcal{E} of the incident light beam. The intensity of fluorescent light is found to be a minimum at zero magnetic field and to increase to a saturation value at high magnetic field.

Classical Treatment

Hanle proposed a simple classical model to account for these findings. The electric vector of the light excites an elastically bound electron of the atom and puts it into oscillation with a direction initially coinciding with \mathcal{E} . The oscillating electron then emits

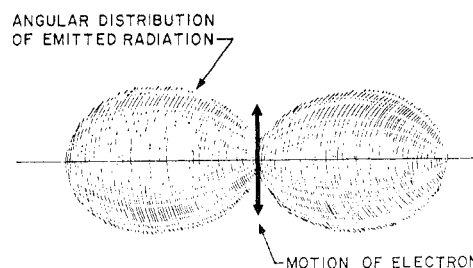


Figure 2. Radiation pattern of light from an oscillating elastically bound electron excited by linearly polarized light. The distribution is cylindrically symmetric about the vertical axis (from Jackson¹²).

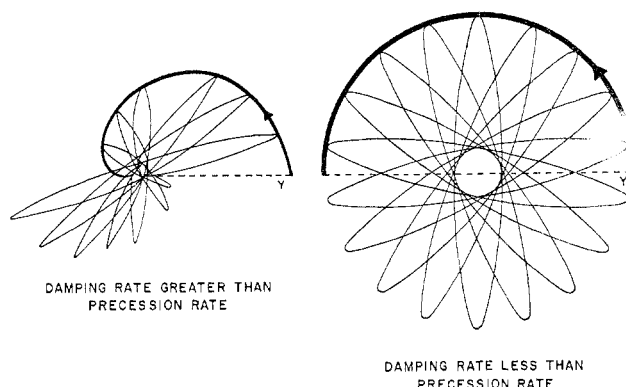


Figure 3. The orbit of an electron initially excited along the y axis executing Larmor precession about a magnetic field perpendicular to the plane of the figure. Shown is one half-turn. Note that the degree of polarization of the fluorescent light is controlled by the competition between the rate of spontaneous emission and the rate of Larmor precession (from Hanle¹¹).

radiation according to the laws of classical electrodynamics. Because of the loss of energy carried off by the radiation field, the motion of the electron is continually being damped, thus causing the amplitude of its oscillation to be reduced until the electron once again comes to rest. In the absence of a magnetic field, then, the fluorescent radiation is polarized with a cosine-squared radiation pattern, which is characteristic of a dipole antenna¹² (see Figure 2). An observer viewing this dipole oscillator head-on sees no radiation, whereas an observer viewing at right angles to the dipole axis sees a maximum.

In the presence of a magnetic field, there is a torque exerted on the electron by virtue of its orbital motion. The oscillating electron is caused to precess about the magnetic field, and its orbit describes a rosette (see Figure 3). As the oscillating dipole radiates, the polarization of the light detected by a stationary observer in the laboratory decreases until, at sufficiently high magnetic field, the electron, on the average, makes so many revolutions before radiating that the fluorescence appears to be completely depolarized. Further increases in the magnetic field strength then have no additional effect on the fluorescent polarization.

Let us sharpen this pictorial description by restating it in mathematical terms. Let the incident light beam

(12) See J. D. Jackson, "Classical Electrodynamics," Wiley, New York, N. Y., 1962, Chapters 9, 16, and 17.

propagate along the x axis, with its electric vector pointing along the y axis. The magnetic field direction then defines the z axis (see Figure 1). At time $t = 0$, we suppose the system absorbs a photon, thereby starting an electric dipole to oscillate in the initial direction of the y axis. At a subsequent time t , the oscillator has rotated in the xy plane by an angle $\varphi = \pi/2 + \omega t$, here the azimuthal angle φ is measured from the x axis. The precession frequency ω is equal to $\mu_0 g H / \hbar$, where μ_0 is the electronic Bohr magneton. The term g is the Landé factor expressing the quotient of the magnitude of the average magnetic moment along the total angular momentum divided by the magnitude of the total angular momentum of the system. Because of the exponential decay of the fluorescence, the amplitude of the dipole oscillator must also be diminished by a factor $\exp(-t/2\tau)$, where τ is the lifetime of the excited state. The intensity detected along the y axis with a polarization parallel to the x axis, $I_y(\mathcal{E}_x, t)$, is proportional to the square of the amplitude of the projection of the dipole oscillator along the x axis. Hence, we have the condition

$$I_y(\mathcal{E}_x, t) = C \sin^2(\mu_0 g H t / \hbar) \exp(-t/\tau) \quad (1)$$

where C is a proportionality constant. Note that the time dependence of the fluorescent light emission from a light pulse received at $t = 0$ results in an exponential decay modulated at the Larmor precession frequency.¹³

For steady-state illumination, the intensity recorded by the detector is a sum over all possible elapsed time intervals t and is given by eq 2. If the observed in-

$$I_y(\mathcal{E}_x) = C \int_0^\infty \sin^2(\mu_0 g H t / \hbar) \exp(-t/\tau) dt = \\ (1/2) C \tau (2\mu_0 g \tau H / \hbar)^2 / [1 + (2\mu_0 g \tau H / \hbar)^2] \quad (2)$$

tensity, $I_y(\mathcal{E}_x)$, is plotted as a function of magnetic field strength H , the Hanle-effect signal has a Lorentzian shape with a half-width at half-maximum of

$$H_{1/2} = \hbar / 2\mu_0 g \tau \quad (3)$$

Thus by determining the value of $H_{1/2}$ the Hanle effect permits the measurement of the product $g\tau$.

It should be noted that this classical derivation is applicable to molecules as well as atoms and depends on the validity of describing the resonance fluorescence process by absorption dipole oscillators. Of course, for molecules the directions of the absorption and emission dipole oscillators need not coincide, and the internal motions of the molecule, such as rotation and, in the case of polyatomics, vibration, may reduce the apparent polarization of the molecular fluores-

(13) A beautiful experimental verification of this prediction has been obtained by J. N. Dodd, W. J. Sandle, and D. Zisserman, *Proc. Phys. Soc. London*, **92**, 497 (1967), who used pulse excitation.

As an alternative to using a pulse of light whose duration is short as compared to the Larmor precession period, the dipole oscillators may also be forced to precess in phase if the incident light is modulated at the Larmor frequency or some multiple thereof, resulting in an enhancement of the modulation amplitude of the reemitted light. See A. Corney and G. W. Series, *Proc. Phys. Soc. London*, **83**, 207, 213 (1964); **84**, 176 (1964).

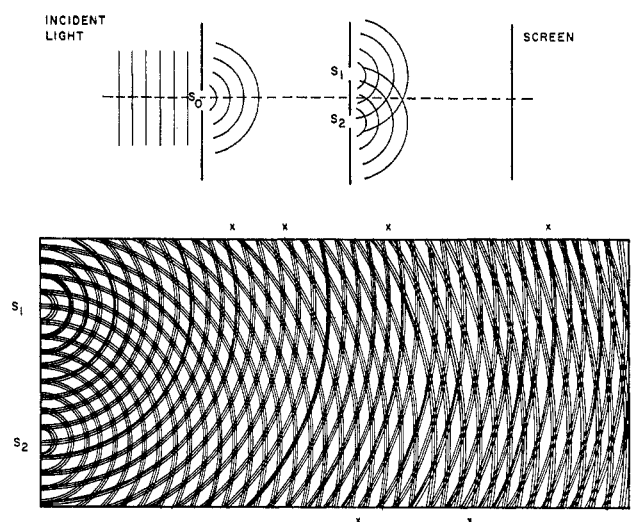


Figure 4. Young's double-slit experiment: (a) optical arrangement for producing an interference pattern by allowing light from slits S_1 and S_2 to fall on a screen; (b) the overlapping of the wavelets from S_1 and S_2 (from Young¹⁶).

cence.¹⁴ Nevertheless, provided the resonance fluorescence is polarized, we may expect the qualitative results of the classical treatment to hold. Moreover, it should also be apparent that we could replace the variable magnetic field by a variable electric field. A Hanle-effect experiment under these conditions would then measure the product of the lifetime τ with the electric moment of the excited state.

Quantum Treatment

To gain a deeper understanding of the nature of interference effects in molecular fluorescence, we must seek the quantum counterpart of eq 1-3. Perhaps it is simplest to start by reviewing the celebrated¹⁵ double-slit experiment of Young¹⁶ shown in Figure 4. Here monochromatic light emerges from a source, S_0 , and passes through two slits, S_1 and S_2 . The two sets of cylindrical wavelets emerging from S_1 and S_2 interfere with each other and form a pattern of bright and dark fringes on a screen. Shown in the lower portion of Figure 4 is a reproduction of Young's original drawing, illustrating interference effects caused by the overlapping waves. By viewing this at a grazing angle with the eye at the extreme left or right edge of the figure it is possible to see along the lines marked by X's a dark region caused by cancellation. In between there is a light region caused by reinforcement.

An analysis of Young's double-slit experiment shows that a fundamental requirement for the existence of interference fringes on the screen in Figure 4 is that the light from the source S_0 must be capable of arriving at a point P on the screen by two distinct paths, *i.e.*,

(14) R. N. Zare, *J. Chem. Phys.*, **45**, 4510 (1966).

(15) It is unclear whether the double-slit experiment is more celebrated for causing confusion or for illustrating interference effects. For a further discussion of this experiment, see F. A. Jenkins and H. E. White, "Fundamentals of Optics," 3rd ed, McGraw-Hill, New York, N. Y., 1957, Chapters 13 and 16.

(16) T. Young, *Phil. Trans. Roy. Soc. London*, **92**, 12, 387 (1802); **94**, 1 (1804); "A Course of Lectures on Natural Philosophy and the Mechanical Arts," Vol. I, Plate XX, London, 1807.

the two slits can "share" the same photon. The intensity at point P is related classically to the square of the electric field strength. The electric fields contributed by each light path must be added together vectorially, and the sum must then be squared to obtain the intensity. Because of the phase difference between the two paths, there are cross-terms in the square of the electric field amplitude, and these cause interference effects. Thus the sharpness of the interference fringes depends on the extent to which the intensity of the light arriving at point P *cannot* be regarded as the sum of the intensities from the two slits. Moreover, it is found that the interference effects are most marked when the two slits for some fixed slit width are close together, but these effects decrease in contrast as the distance between the slits is increased.

We inquire next: what should be the analog of slits in molecular fluorescence; what determines their widths; and what determines their separation?

Let us concentrate our attention on a quantum mechanical system (atom, molecule, crystal) having well-defined angular momentum states, where the axis of quantization is chosen along the magnetic field direction. We suppose that some initial (J, M) , excited (J', M') , and final (J'', M'') states are connected to each other by electric dipole transitions. The final state may or may not be the same as the initial state. The resonance fluorescence process may be regarded as a two-step sequence for our purposes: first absorption $(J, M) \rightarrow (J', M')$; then emission $(J', M') \rightarrow (J'', M'')$. According to the electric dipole selection rules, the change in the magnetic quantum numbers must obey the relation $\Delta M = 0, \pm 1$. In particular, the following polarization rules¹⁷ apply to absorption and emission. For $\Delta M = 0$ transitions, the radiation is linearly polarized with its electric vector along the magnetic field (π light); for $\Delta M = +1$ or $\Delta M = -1$ transitions, the radiation is right- or left-circularly polarized with its electric vector rotating clockwise or counterclockwise in a plane perpendicular to the magnetic field (σ^+ or σ^- light).

Suppose this quantum mechanical system is irradiated with resonance light whose polarization is not pure π , pure σ^+ , or pure σ^- , but rather a linear combination of these. To be specific, we choose the light to be linearly polarized along the y axis, as in Figure 1. This corresponds to an equal superposition of σ^+ and σ^- light with a fixed 180° phase difference. We wish to follow the resonance fluorescence process, concentrating our attention on how one magnetic sublevel of the initial state participates. This is illustrated in Figure 5. The linearly polarized light induces transitions to two possible excited-state sublevels, which in turn decay to three possible final-state sublevels. As a result, two different routes are permitted for the system to undergo the transition $(J, M) \rightarrow (J'', M)$ via the resonance fluorescence process. The probability for the $(J, M) \rightarrow (J'', M)$ transition is given

(17) L. Pauling and E. B. Wilson, "Introduction to Quantum Mechanics," McGraw-Hill, New York, N. Y., 1935, p 308.

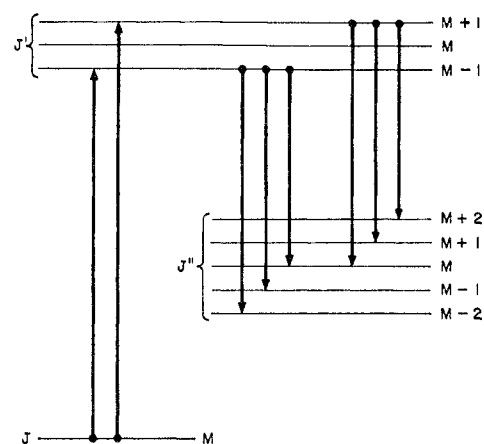


Figure 5. Generation of interference effects through the resonance fluorescence process.

by the square of the sum of the probability amplitudes for the two different paths and thus contains cross-terms which once again cause interference effects. The excited-state sublevels, $(J', M + 1)$ and $(J', M - 1)$, may be said to "share" the same photon, and their radiative decay patterns interfere with each other, causing the distribution of the fluorescent light to be anisotropic.

We now have answered the questions previously posed: the magnetic sublevels of the excited state play the role of slits in the resonance fluorescence process; the slit widths correspond to the broadening of the energy levels because of the finite lifetime of the excited state; and the slit separations are given by the Zeeman splitting of these sublevels in the magnetic field. By analogy with the two-slit experiment, we should find the interference pattern to be most pronounced when the slits are closest together and to disappear gradually as the slits are moved apart.

Let us use the uncertainty principle

$$\Delta E \Delta t = \hbar \quad (4)$$

to make an estimate of the Hanle-effect line width, $H_{1/2}$. In eq 4 the energy separation ΔE is given by $\mu_0 g(M + 1)H_{1/2} - \mu_0 g(M - 1)H_{1/2}$, i.e., by $2\mu_0 gH_{1/2}$. For the uncertainty in the time Δt we shall use the lifetime τ . Substitution in eq 4 then yields eq 5, with the same

$$H_{1/2} = \hbar / 2\mu_0 g \tau \quad (5)$$

result as in eq 3. Of course, an appeal to the uncertainty principle is dandy for an order-of-magnitude estimate but should not be expected to give the exact answer. For example, it is seldom apparent whether one ought to write eq 4 with h or \hbar . Hence we must regard the agreement between eq 3 and 5 as fortuitous, or, more cynically, as a swindle by someone who already knows what he wants to see. Nevertheless, this encourages us to attempt a somewhat more full-blown quantum treatment.

We return to the resonance fluorescence process shown in Figure 5. For absorption of light plane polarized along the x axis, the excited-state wave function can be written as eq 6, whereas, for absorption

$$|x\rangle = (-1/\sqrt{2})[a_{M+1}|M+1\rangle + a_{M-1}|M-1\rangle] \quad (6)$$

of light plane polarized along the y axis, the excited-state wave function has the form of eq 7. Note that

$$|y\rangle = (-i/\sqrt{2})[a_{M+1}|M+1\rangle - a_{M-1}|M-1\rangle] \quad (7)$$

$|x\rangle$ and $|y\rangle$ are "mixed" states which are a coherent superposition of eigenstates; they differ from each other by their relative phases. The coefficients a_M are proportional to the electric dipole matrix element connecting the ground-state sublevel (J, M) to the excited-state sublevel (J', M').

The incident light will excite the system at time $t = 0$ to a level $|\Psi_{\text{ex}}\rangle$, which is initially identical to $|y\rangle$.¹⁸ The time development of $|\Psi_{\text{ex}}\rangle$ is governed by the Schrödinger equation (eq 8), which has the formal

$$(-\hbar/i)(d/dt)|\Psi_{\text{ex}}\rangle = \mathcal{H}|\Psi_{\text{ex}}\rangle \quad (8)$$

solution

$$|\Psi_{\text{ex}}(t)\rangle = [\exp(-i\mathcal{H}t/\hbar)]|\Psi_{\text{ex}}(t=0)\rangle \quad (9)$$

where $\exp(-i\mathcal{H}t/\hbar)$ is to be interpreted as the power-series expansion. Actually, eq 9 is incomplete, for it ignores the radiative decay of the excited state. We may include spontaneous emission in a semiclassical manner by changing eq 9 to read

$$|\psi_{\text{ex}}(t)\rangle = [\exp(-t/2\tau)][\exp(-i\mathcal{H}t/\hbar)]|\Psi_{\text{ex}}(t=0)\rangle \quad (10)$$

Since the excited-state eigenvalues are $E_0 + \mu_0 g M H$, we find that we have the condition

$$\begin{aligned} |\Psi_{\text{ex}}(t)\rangle &= (-i/\sqrt{2}) \exp(-t/2\tau) \exp(-i\mathcal{H}t/\hbar) \times \\ &\quad [a_{M+1}|M+1\rangle - a_{M-1}|M-1\rangle] \\ &= (-i/\sqrt{2}) \exp(-t/2\tau) \exp[-i(E_0 + \\ &\quad \mu_0 g M H)t/\hbar] [a_{M+1} \exp(-i\mu_0 g H t/\hbar)|M+1\rangle - \\ &\quad a_{M-1} \exp(i\mu_0 g H t/\hbar)|M-1\rangle] \\ &= \exp(-t/2\tau) \exp[-i(E_0 + \mu_0 g M H)t/\hbar] \times \\ &\quad [|x\rangle \sin(\mu_0 g H t/\hbar) + |y\rangle \cos(\mu_0 g H t/\hbar)] \quad (11) \end{aligned}$$

Equation 11 has the simple physical interpretation that the excited state of the system changes continuously from $|y\rangle$ to $|x\rangle$ and then back to $|y\rangle$, etc., at the Larmor precession frequency. The mixed states $|x\rangle$ and $|y\rangle$ are the quantum analogs of the x - and y -directed dipole oscillators.

Note that light polarized with its electric vector along the x axis can only come from the $|x\rangle$ component of the excited-state wave function. Thus the intensity of emitted light plane polarized in the x direction is given by the square of the amplitude of the x component (eq 12) and the steady-state fluorescence is

$$I_y(\mathcal{E}_x, t) = C \exp(-t/\tau) \sin^2(\mu_0 g H t/\hbar) \quad (12)$$

(18) The assumption that excitation occurs at some instant of time needs some justification. In particular, this treatment is valid for broad-band excitation, *i.e.*, when the spectral profile of the incident light is sufficiently wide for it to excite simultaneously the excited-state sublevels. Moreover it may be shown for almost perfectly monochromatic light, such as that from lasers, that the treatment is still justified, provided the Doppler width exceeds the natural width.

found by integrating this expression over all time intervals t .

$$I_y(\mathcal{E}_x, t) = (1/2)C\tau(2\mu_0 g \tau H/\hbar)^2/[1 + (2\mu_0 g \tau H/\hbar)^2] \quad (13)$$

Equations 12 and 13 are, of course, identical with eq 2 and 3.

A simple generalization of this treatment including the contributions from all the ground-state sublevels (which we assume to be equally populated with random phases) yields expression 14, where P represents the

$$\begin{aligned} I_y(\mathcal{E}_x) &= K \sum_M \sum_{M''} \sum_{M'} \sum_{M_2'} \langle J'M_1' | P_y | JM \rangle \langle JM | P_y | J'M_2' \rangle \times \\ &\quad \langle J'M_1' | P_x | J''M \rangle \langle J''M | P_x | J'M_1' \rangle / \{1 + \\ &\quad [(E_{M_2} - E_{M_1})\tau/\hbar]^2\} \quad (14) \end{aligned}$$

transition dipole moment operator, and K is a proportionality constant. Equation 14 is a special case (appropriate to the geometry shown in Figure 1) of a formula first given by Breit¹⁹ and later derived more simply by Franken.²⁰

The magnetic moment of a molecule has the same origin as that of an atom, namely, in both cases the magnetic moment arises from the orbital and spin angular momentum of the electron. Thus a molecule may be regarded as a "bottled" free electron, and the magnitude of the g factor tells us about the nature of the bottle. Because of the different angular-momentum coupling schemes in molecular excited states and their marked dependence on the rotational quantum number J , the molecular g factors have a wide spread in values, as do the molecular radiative lifetimes. For example, for the $v' = 0, N' = 2, J' = 3/2$ level of the OH A $2\Sigma^+$ state, we determined $H_{1/2}$ to be 0.258 ± 0.036 G,⁴ whereas for the $v' = 10, J' = 12$ level of the Na₂ B $1\Pi_u$ state, we found $H_{1/2} = 1385 \pm 42$ G.⁸

High-Field Level Crossings and Anticrossings

We see from the preceding that the interference effects in the fluorescent intensity are greatest when the energy levels E_{M_1}, E_{M_2} are degenerate, *i.e.*, "crossed," but they disappear as the interference energy levels E_{M_1}, E_{M_2} became well resolved ("uncrossed") with respect to their natural widths. Thus, the Hanle effect can be thought of as arising from the intersection or crossing of magnetic sublevels at zero field, and is often referred to as zero-field level crossing. When hyperfine structure is present or when the fine structure splittings are small, intersections of magnetic sublevels may occur at nonzero values of the magnetic (or electric) field; these are referred to as high-field level crossings.²¹ Of course, not every crossing of two mag-

(19) G. Breit, *Rev. Mod. Phys.*, **5**, 91 (1933).

(20) P. A. Franken, *Phys. Rev.*, **121**, 508 (1961).

(21) The first instance of this was the observation by F. D. Colegrave, P. A. Franken, R. R. Lewis, and R. H. Sands, *Phys. Rev. Lett.*, **3**, 420 (1959), on the 2^3P fine structure of helium. So far, no high-field level crossings have been detected for molecular systems, although there is nothing to prevent the observation of such phenomena. NOTE ADDED IN PROOF. Recently, Dr. E. M. Weinstock of our laboratory has found a high-field level crossing in the $A^2\Sigma^+$ state of OD.

netic sublevels will alter the detected fluorescence intensities. Indeed, to observe interference effects in the fluorescence, two conditions must be met: (1) in the excitation process the excited state is placed into a coherent superposition state, *e.g.*, by excitation with a mode of polarization that is capable of stimulating at least two different transitions from the same initial state; (2) the fluorescent light which reaches the detector must have arisen from the decay of these two transitions to some common final state.

Further consideration shows that it is not necessary for the two excited-state sublevels to actually cross. Interference effects can still be observed if the two levels approach each other closely enough for them to overlap within their natural widths.²² Then one of the energy-denominator terms in the Breit level-crossing formula will be quite small, causing an anomaly to appear in the angular distribution of the reemitted light. By measuring a sufficient number of high-field crossings or anticrossings, it is possible to extract from the data the energy-level pattern of the excited state.

Optical Radiofrequency Double Resonance

So far the methods we have discussed permit us to determine the product of the lifetime and the energy difference between two sublevels that can be coherently excited. Of course, if one of these two factors is known independently by other means, then the width of the level-crossing signal can be used to find the other factor. However, for most molecular excited states, little is known about the rate of spontaneous emission or the nature of the energy-level pattern. In such cases another interference technique, based on inducing radiofrequency resonances between the excited-state sublevels, becomes quite useful. It is well known that rf photons are "fat, flabby, and indiscrete," whereas optical photons are "strong, skinny, and discrete," *i.e.*, $(h\nu)_{\text{rf}} \ll (h\nu)_{\text{optical}}$. Consequently, rf transitions in the gas phase cannot be readily detected by direct measurement of the absorption or emission of rf power. However, by altering the fluorescent radiation pattern, it is possible to monitor the rf transitions through the optical emission of the molecules. This is the basic idea behind optical double resonance.²³

Figure 6 pictures a typical double-resonance experiment. Here we use π optical excitation, in which the light beam is incident along the x axis with its electric vector along the magnetic field (z axis). We apply an rf field \mathbf{H}_1 which rotates at frequency ω_1 in the xy plane. When ω_1 is not commensurate with the Larmor precession frequency, ω , the rf field rapidly oscillates in and out of phase with the precessing electric dipoles. The reemitted light is then unaffected by the rf field and is π polarized. However, when $\omega_1 \cong \omega$, the rf field rotates in phase with the precessing dipoles

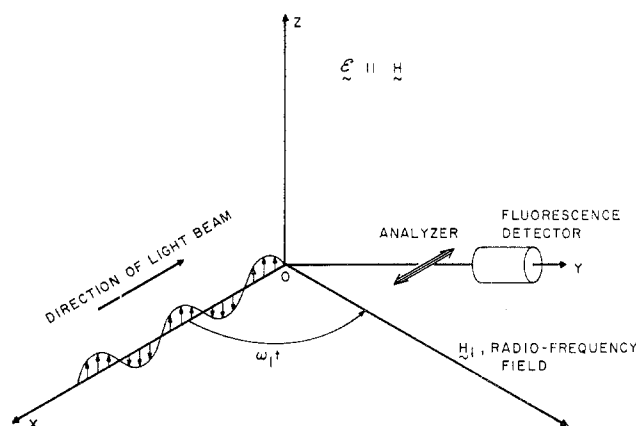


Figure 6. The optical double-resonance experiment.

and induces transitions among the magnetic sublevels. This causes σ components to appear in the reemitted light. The width of the resonance (at low rf powers) is again found to be the natural width of the excited state.²⁴ By measuring the frequency, ω_1 , of the rf field and the strength of the static external field, we then obtain a value for the energy-level difference that is independent of the excited-state lifetime.

The resonance condition, $\omega_1 = \omega$, is particularly instructive. Consider an observer who "rides" with \mathbf{H}_1 in the xy plane. In this rotating frame, the effective magnetic field along Oz is zero at resonance; the only field experienced by the observer is \mathbf{H}_1 . Thus, the setup shown in Figure 6 corresponds to performing at resonance a Hanle-effect experiment in the rotating frame.²⁵ In terms of our classical model, the dipole oscillator is first excited along Oz . In the initial stages of its motion, the dipole oscillator is unaffected by \mathbf{H} but is entirely controlled by \mathbf{H}_1 . The \mathbf{H}_1 field causes the oscillator to execute rosette motion in a plane perpendicular to \mathbf{H}_1 , but this plane (driven by \mathbf{H}_1) precesses about \mathbf{H} at the Larmor frequency. To a stationary observer in the laboratory frame, the fluorescence light at resonance then has σ as well as π polarization and appears to be 100% modulated at twice the Larmor frequency.

Application to Molecular Systems

Excited states of molecules have conventionally been studied by optical spectroscopy either in absorption or in emission. The precision of such work cannot exceed the Doppler width of the lines, typically 0.04 cm^{-1} , caused by the translational motion of the molecules. However, the precision achieved by the use of interference techniques as described above is limited only by the natural width of the lines. For a typical molecular lifetime spread of 10^{-6} to 10^{-8} sec, this corresponds to a resolution of 0.0001 to 0.01 cm^{-1} . This gain in precision is very considerable and permits information to be obtained about the nature of molecu-

(22) See K. C. Brog, T. G. Eck, and H. Wieder, *Phys. Rev.*, **153**, 91 (1967); H. Wieder and T. G. Eck, *ibid.*, **153**, 103 (1967).

(23) The first optical double-resonance experiments were performed on the 3P_1 state of Hg by J. Brossel and F. Bitter, *ibid.*, **86**, 308 (1952). So far, optical double-resonance studies have been performed on the molecules CS, OH, and OD.

(24) J. N. Dodd and G. W. Series, *Proc. Roy. Soc., Ser. A*, **263**, 353 (1961).

(25) Indeed, level-crossing measurements may be regarded as optical double-resonance measurements at zero radiofrequency.

lar excited states which heretofore would have escaped detection. This in turn allows us to make a comparison between the value of the excited-state coupling parameter determined by experiment and the value predicted by quantum chemistry calculations. Presently, our knowledge of the structure of short-lived excited states of molecules is exceedingly primitive compared to that of ground states. The methods of level-crossing and optical double-resonance experiments permit us to study excited states with a precision approaching that of microwave, esr, and molecular-beam resonance studies of ground and metastable states. As with almost all molecular spectroscopy, the contribution of these interference methods to our chemical understanding seldom comes from one mea-

surement, but rather is a cumulative process depending upon our ability to interpret the trends that emerge in terms of "chemical shifts," used in the broadest sense of the meaning. The application of interference techniques to probe the charge distributions of molecular excited states is a fairly recent development. Already, as shown in Table I, excitation by atomic line coincidences, molecular resonance lamps, white light sources, selected laser lines, and even electron impact has proven successful in stimulating interference effects in molecular emissions. As additional means are found to extend these techniques to transient molecular species, the field may be expected to grow rapidly.

Support by the National Science Foundation is gratefully acknowledged.

Some Aspects of Small-Angle X-Ray Scattering

GEORGE W. BRADY

Bell Laboratories, Murray Hill, New Jersey 07974

Received January 11, 1971

In this Account we will discuss the techniques of small-angle X-ray scattering as applied to structural problems of the liquid state. There are, of course, other areas in which the method is of great use,¹⁻³ but we will limit ourselves to the studies of inhomogeneities in liquids and of scattering phenomena which occur at or near critical points and phase transitions.

As its name implies, small-angle scattering designates that part of the intensity pattern which is observed in the vicinity of the main beam. Its angular limits will be defined later. It was first noticed or reported in the 1930's, notably by Bernal⁴ and coworkers in their work on tobacco mosaic virus, and by Krishnamurti and Warren,⁵ who studied carbon black. The first detailed investigation of the phenomenon was made by Guinier,⁶⁻⁸ who was interested in studying that part of the X-ray intensity pattern which lies between the Bragg peaks.

To do this, great care had to be taken to remove all extraneous scattering from the weak intensity patterns, and it was an experimental triumph when Guinier's painstaking efforts brought this about. One of the main sources of this unwanted scattering was the presence of the continuous spectrum in the target beam.

(1) The literature on small angle scattering has grown large, but strangely enough the only textbook in the field, "Small Angle Scattering of X-Rays," by Guinier, *et al.*, J. Wiley and Sons, New York, 1955, is out of print. The best survey of the field up to 1965 is given in ref 2. An up-to-date bibliography is given in ref 3.

(2) H. Brumberger, Ed., "Small Angle X-Ray Scattering," Gordon and Breach, New York, London, and Paris, 1967.

(3) A. J. Renouprez, *Int. Union Crystallogr., Comm. Crystallogr. App., Bibliogr.*, No. 4 (1970).

(4) J. D. Bernal and I. Fankuchen, *J. Gen. Physiol.*, **25**, 111 (1941).

(5) P. Krishnamurti, *Indian J. Phys.*, **5**, 473 (1930); B. E. Warren, *J. Chem. Phys.*, **2**, 551 (1934).

(6) A. Guinier, *C. R. Acad. Sci.*, **206**, 1641 (1938).

(7) A. Guinier, *Ann. Phys. (Paris)*, **12**, 161 (1939).

(8) A. Guinier, *Phys. Today*, **22**, 25 (1969); see also ref 1-3.

To isolate the characteristic $K\alpha$ line and still obtain sufficient intensity, a curved crystal monochromator had to be used. This had the added result of focusing the incident beam to a small angle, thus allowing the isolation of a scattered spectrum which was centered around zero. Elimination of air and slit scattering further reduced the background.

After the carbon black measurements of Warren were confirmed, a search for the origin of the scattering was begun. A study of silica in the vitreous state (no small-angle scattering) and in a gel (small-angle scattering) indicated immediately that the scattering arose from inhomogeneities of a mean size much greater than that of interatomic spacings (which give rise to the usual Bragg peaks). In fact, they were of the order of the grain size of the silica gel.

This result demonstrated for the first time that X-rays could be used for determination of the morphology of relatively large aggregates or molecules, of the order of tens to thousands of ångströms.

Guinier⁸ soon developed a theory for the phenomenon which gave a simple relation between the intensity and the radius of gyration \bar{R} . \bar{R} is the average distance of the electron density distribution from the center of charge. Thus for a large molecule or particle

$$\bar{R}^2 = \frac{\int \rho(r)r^2 dv}{\int \rho(r) dv} \quad (1)$$

where $\rho(r)$ is the electron density at a distance r and v is the volume of the particle. The relation is

$$I \sim e^{-s^2 \bar{R}^2/3} \quad (2)$$

where $s = 4\pi/\lambda \sin \theta$; λ is the wavelength, and θ is one-half the scattering angle.